Chapter 3

Torque Ripple Reduction in DSSRM

3.1 Introduction

SRMs possess a high torque ripple because of the salient pole structure and discrete excitation of phases. In the literature, different types of active and passive torque ripple reduction techniques have been proposed to reduce the torque ripple in different SRM topologies. In an active method , the shaping of phase currents through an electronic controller is employed to reduce the torque ripple. On the contrary, in a passive method, a change in the magnetic characteristics of the machine is introduced via structural modifications to reduce the torque ripple.

The main region of torque ripple in DSSRMs is during the commutation of the outgoing phase. In this region, the outgoing and incoming phases both have reduced torque production. Due to this, the resultant torque has a large dip in this region, resulting in a high torque ripple. In this chapter, the angular shift in rotor segments and stator/rotor surfaces have been investigated to reduce the torque ripple in single-tooth winding DSSRM. In this regard, the chapter is structured as follow: Section 3.2 defines a schematic for torque ripple reduction. Section 3.3 utilizes this schematic to investigate the torque ripple mitigation in the considered DSSRM topology through rotor segments shift. In Section 3.4, the shift in the stator and rotor surfaces are studied for torque ripple mitigation in DSSRM. Finally, Section 3.5 concludes the chapter.

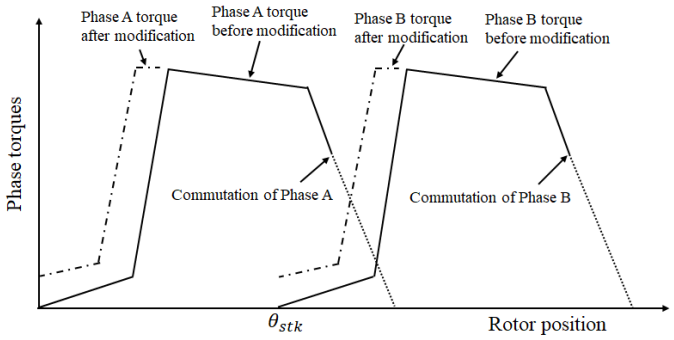

(a)

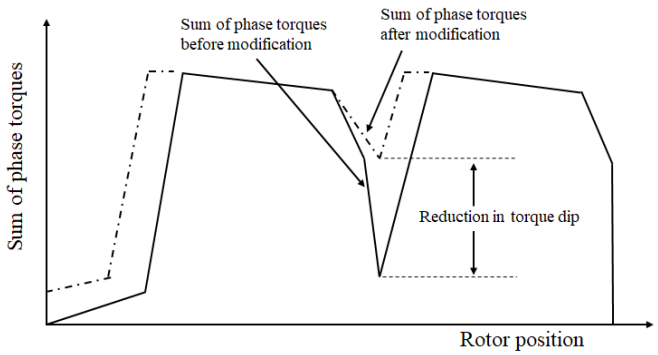

(b)

Figure 3.1: Schematic for torque ripple reduction. (a) Phase torques. (b) Sum of phase torques.

3.2 Schematic for torque ripple reduction in DSSRM

The main region of torque ripple generation in SRMs is during the commutation of the outgoing phase. During this period, the torque shared by the outgoing phase reduces significantly. However, at the same time, the value of $dL/d\theta$ is less for the incoming phase. Because of this, the torque generated by the incoming phase is also less in this region. This phenomenon results in a large torque dip and subsequently large torque ripples in this region. Fig. 3.1 shows the pictorial representation of this phenomenon. Fig. 3.1 (a) shows the typical static torque profiles of two consecutive phases; phase A and phase B (solid lines) which are separated by the stroke angle θ_{stk}. Here, phase A can be considered as outgoing phase whereas phase B as incoming phase. When phase A is commutated, it is assumed that the torque contributed by this phase becomes negligible immediately. At the same time, phase B operates as the incoming phase and has not achieved sufficient torque generation. Fig. 3.1 (b) shows the sum of these torques (solid

line) considering the commutation effect. It is seen that a large torque dip is created in this region which results in a high torque ripple in the motor. However, suppose any structural modification is introduced in the machine in such a way that the incoming phase has increased torque generation in this region. In that case, the torque dip will reduce, which subsequently reduces the torque ripple. In Fig. 3.1 (a) and Fig. 3.1 (b), the dot-dash lines show the proposed phase torques and sum of the phase torques, respectively, after such modifications. It can be seen that in the case of modified structure, the incoming phase has increased torque generation in the commutation region, resulting in low ripples in output torque.

3.3 Torque ripple reduction through rotor segments shift

In [84, 85], the methods of PM shifting and grouping are discussed to reduce the torque ripple due to the cogging in AFPM motor. In the current study, the angular shift in rotor segments is analysed to reduce the torque ripple in DSSRM. It is observed in FEM based study that shifting of all the rotor segments does not provide a significant reduction in the torque ripple. Therefore, shifting of the alternate rotor segments with an angle of δ in the direction of rotation is discussed here. The proposed design modification is illustrated in Fig 3.2. Fig. 3.2 (a) highlights the placement of the rotor segments in case of an original motor. In this case, the adjacent rotor segments have uniform separation of β_{ro} between them. Fig. 3.2 (b) represents the modified rotor in which the alternate segments viz. S2, S4, S6, S8 and S10 are shifted in the direction of rotation with an angle δ from their original positions. Fig. 3.3 shows the structure of the proposed DSSRM after the segments shift with respect to the exciting poles of the motor. It is seen that for two consecutive exciting poles of a phase, the separation between the adjacent rotor segments is decreased and increased respectively. Therefore, the proposed design modification is valid for the machines with even multiplicity ($m = 2, 4$,...etc.) with the number of rotor segments $N_r = m(4n \pm 1)$; where n is a positive integer number. For the slot/segments combinations discussed in previous chapter (Section 2.3), this design modification is only valid with 12/10 and 12/14 pole combinations. It has been already observed that the 12/10 pole combination has better performance over 12/14 pole machine

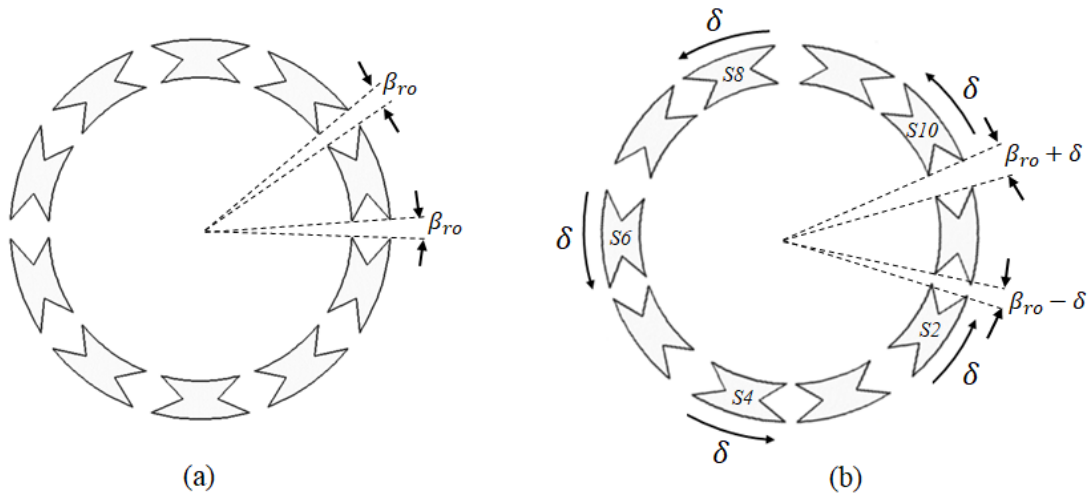

Figure 3.2: Proposed design modification in rotor. (a) Rotor without segments shift (before modification). (b) Rotor with segments shift (after modification).

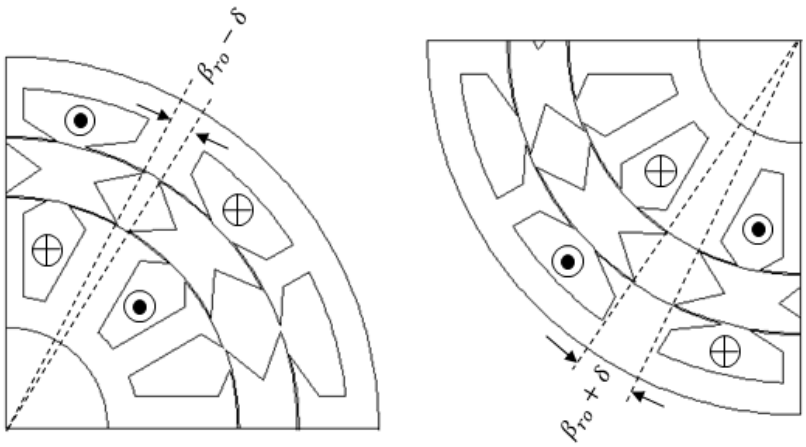

Figure 3.3: Structure of DSSRM with respect to consecutive exciting poles of a phase after the segments shift.

and has already been considered for the analysis in this study. In the case of proposed design modification, the inductance profile of the incoming phase has increased value of $dL/d\theta$ in the commutation region. This increases the torque shared by the incoming phase in this region which reduces torque dip and torque ripple of the motor.

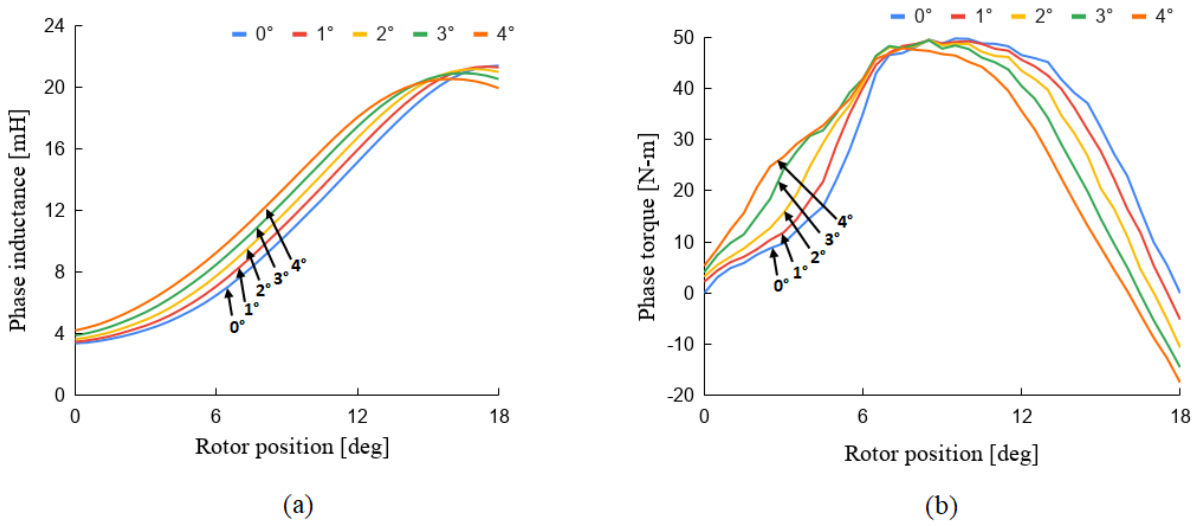

Figure 3.4: Variation in static inductance and static torque profiles of 12/10 pole DSSRM with the variation of segment shift angle (δ). (a) Static inductance. (b) Static torque.

3.3.1 Influence of rotor segments shift on static inductance and torque profiles

The static phase inductance and torque profiles are simulated through FEM procedure in the case of shifted rotor segments. Fig. 3.4 shows the static inductance and static torque profiles of 12/10 pole DSSRM for rated current with the segments shift angle δ between 1°–4°. It is observed in Fig. 3.4 (a) that the value of unaligned inductance and the value of $dL/d\theta$ increase near the unaligned position (here in this case 0° rotor position) with the increase in δ. However, the value of aligned inductance and the value of $dL/d\theta$ reduces near aligned position (here in this case 18° rotor position) with the increase in δ. In Fig. 3.4 (b), it is observed that the phase torque of the machine increases near the unaligned position with the increase in δ. However, with the increase in δ, the phase torque reduces near the aligned rotor position because of the decrease in $dL/d\theta$ in this range.

Fig. 3.5 shows the sum of the static phase torques of phase A and phase B which are separated by the stroke angle (12° in this case) for the value of δ between 1°–4° considering the commutation effect. The phase commutation angle taken is 14.5° (mech). It is assumed that after the commutation of the outgoing phase, the torque contributed by that phase becomes negligible. It is seen in the figure that with the increase in δ between 1°–3°, the torque dip occurring in the commutation region reduces. This is because the torque of the incoming phase increases with the increase in δ, consequently, the sum of

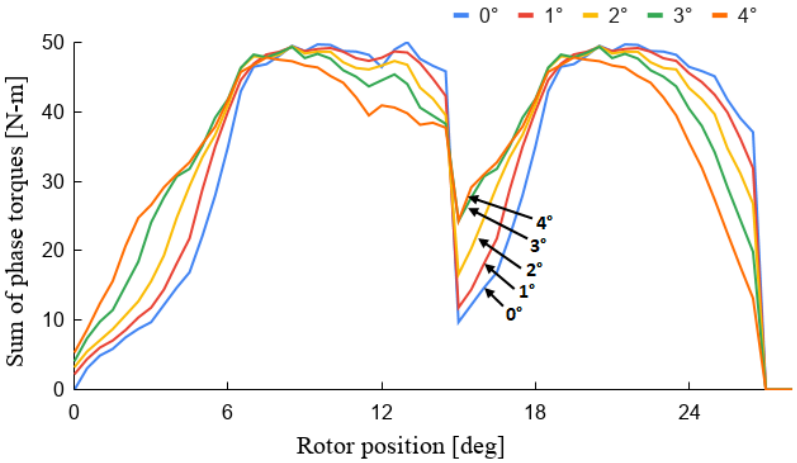

Figure 3.5: Sum of the static phase torques with the shift of the rotor segments showing reduction in torque dip in commutation region.

phase torques increases. However, with the further increase in δ, the reduction in torque dip becomes limited. This is because for the higher value of δ, the reduction in torque of the outgoing phase near aligned rotor position becomes significant over the increase in the torque of incoming phase. Subsequently, the sum of phase torques becomes less significant for torque ripple reduction. The above observations are obtained through the static phase torque profiles. To obtain the more precise results, the dynamic response for the proposed modification is further analyzed through FEM study in the next subsection.

3.3.2 Dynamic response and analysis of torque ripple reduction

The dynamic response of the DSSRM is obtained through FEM based simulation analysis for the value of δ between 0°–4°. The variation in the torque ripple and output torque with the variation δ is shown in Fig. 3.6 for the rated speed. The output torque and torque ripple for the original DSSRM without segments shift ($\delta = 0°$) are 40.1 N-m and 78.5% respectively. With the shift of the rotor segments, the torque ripple starts decreasing. The minimum value of torque ripple is obtained for the shift angle δ of 2.5°. The torque ripple, in this case, is 46.8% with an output torque of 39.3 N-m. Consequently, the torque ripple reduces by 40%, however, the output torque also reduces by 2%. For the further increase in δ, the torque ripple starts increasing and the output torque also reduces considerably. Therefore, the optimal value of δ for the considered 12/10 pole motor is 2.5°. The performace of the motor is further analyzed for this value of δ.

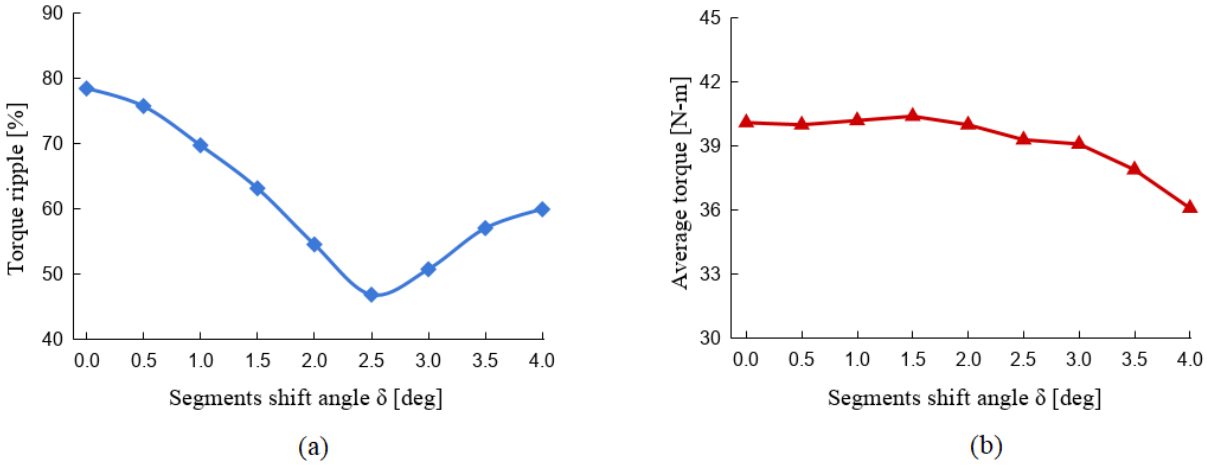

Figure 3.6: Variation of torque ripple and average output torque of 12/10 pole DSSRM with rotor segments shift angle δ. (a) Torque ripple. (b) Average torque.

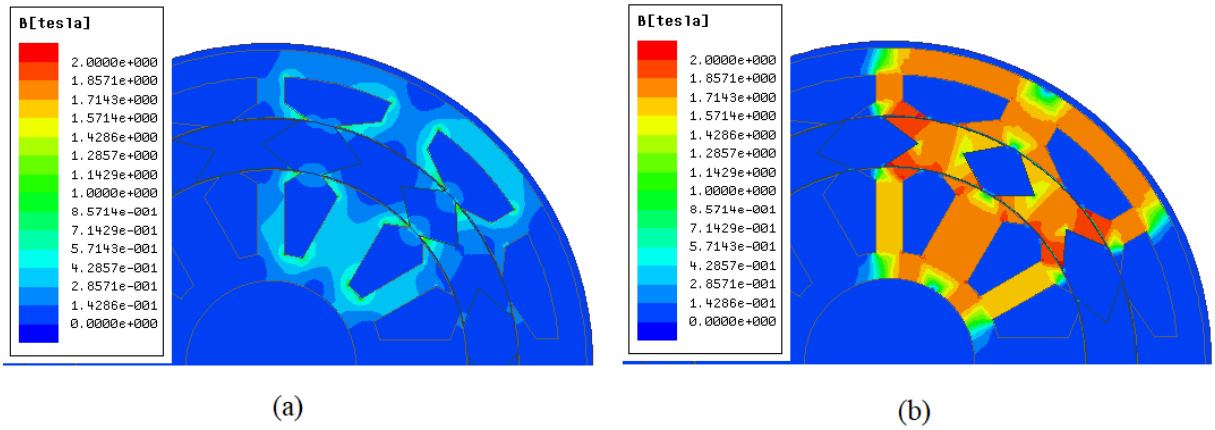

Figure 3.7: Flux density plot in 12/10 pole DSSRM with rotor segments shift ($\delta = 2.5°$). (a) Unaligned position. (b) Aligned position.

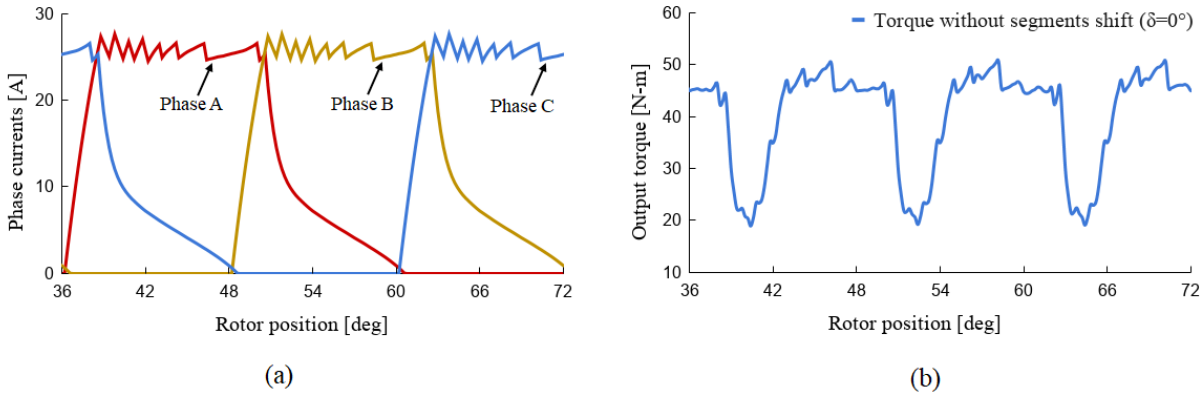

Figure 3.8: Phase currents and torque variation of 12/10 pole DSSRM without segments shift. (a) Phase currents. (b) Dynamic torque.

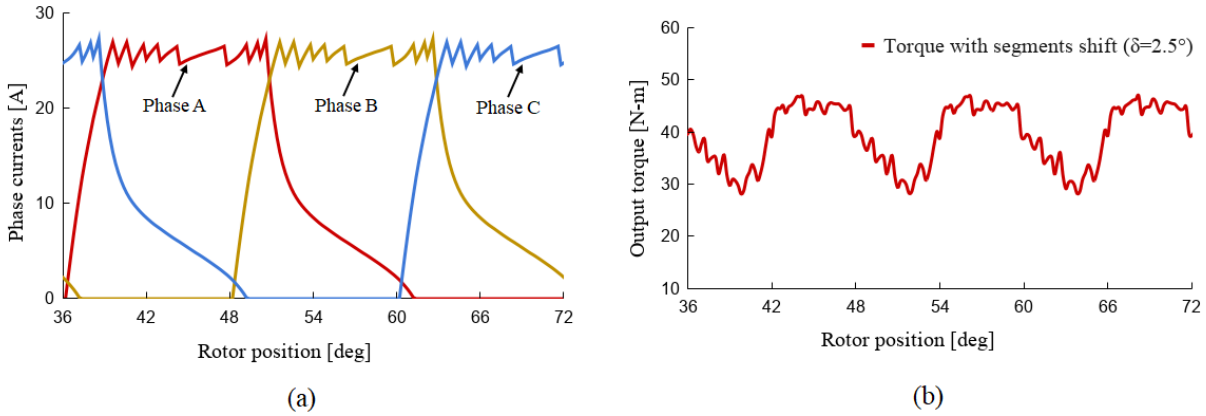

Figure 3.9: Phase currents and torque variation of 12/10 pole DSSRM with segments shift ($\delta = 2.5°$). (a) Phase currents. (b) Dynamic torque.

Fig. 3.7 shows the flux density plot in DSSRM in unaligned and aligned rotor positions, respectively for the case of $\delta = 2.5°$. The peak MMF considered is 1404 AT per slot. Fig. 3.8 and Fig. 3.9 show the steady-state waveforms of phase currents and output torque for the DSSRM without and with rotor segments shift, respectively, at the rated speed. From Fig. 3.8 (b), the average torque, peak-to-peak torque ripple and % torque ripple is found to be 40.1 N-m, 31.5 N-m and 78.5%, respectively, for the DSSRM without segments shift. The above values change to 39.3 N-m, 18.4 N-m and 46.8% respectively for the DSSRM with segments shift ($\delta = 2.5°$), which is shown in Fig. 3.9 (b). Table 3.1 compares the performance data for these cases. It is seen that the torque ripple is reduced by 40% with the shift of rotor segments by 2.5°. However, the output torque is also reduced by 2%. The rated efficiency of the modified machine is 85.4%, which is comparable with the baseline machine. Fig. 3.10 compares the steady-state torques of the DSSRM without and with the rotor segments shift. It is seen that the torque dip occurring in the commutation region reduces in the case of the proposed motor and therefore, the torque ripple decreases. Fig. 3.11 shows the simulated torque-speed characteristics of the modified DSSRM. It is observed that the machine has nearly flat torque profile till the rated speed which is one of the primary requirements in direct drive electric vehicles. Therefore, this machine can be a suitable contender for such applications.

Table 3.1: Performance comparison of 12/10 pole DSSRM without and with rotor segments shift.

Parameter	Without segment shift ($\delta = 0°$)	With segments shift ($\delta = 2.5°$)
Output torque	40.1 N-m	39.3 N-m
Peak-to-peak torque riple	31.5 N-m	18.4 N-m
Torque ripple	78.5%	46.8%
Unaligned inductance	3.53 mH	3.77 mH
Aligned inductance	21.85 mH	21.07 mH
Reduction in torque ripple	-	40%
Reduction in output torque	-	2%
Core loss	53 W	60 W
Copper loss	362 W	362 W
Rated efficiency	85.8%	85.4%

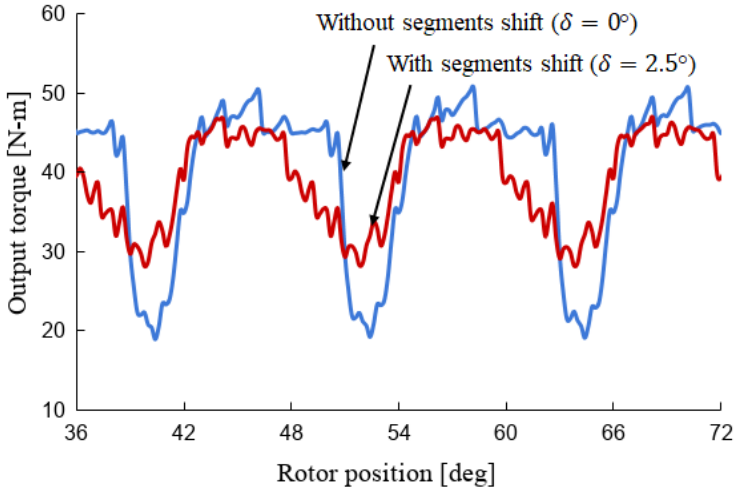

Figure 3.10: Comparison of steady-state torques of 12/10 pole DSSRM without and with rotor segments shift.

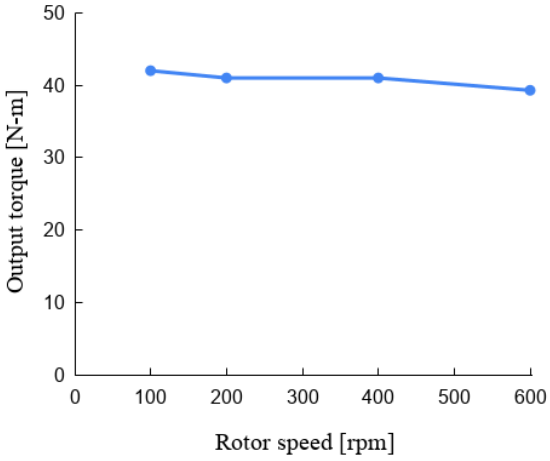

Figure 3.11: Variation of output torque with rotor speed in modified DSSRM ($\delta = 2.5^{\circ}$).

3.3.3 Harmonic analysis of torque ripple frequencies

The torque dip and torque ripple are reduced in the case of DSSRM with the alternate rotor segments shift which can be observed in Fig 3.10. The harmonics spectrum of various frequencies of the dynamic output torque without and with rotor segments shift is calculated and shown in Fig. 3.12. The average or DC value of the output torques are 40.1 N-m and 39.3 N-m, respectively, without and with rotor segments shift. The fundamental frequency of torque ripple for both the machines is 300 Hz which is also the most dominant harmonic. The magnitude of this harmonic is 28.5% and 19.8% of the output torque in the case of without and with the rotor segments shift, respectively. Therefore, there is an 8.7% reduction in fundamental torque ripple in the modified motor. For the second harmonic, these values are 16.3% and 4.7%, respectively, which shows an 11.6% reduction for this harmonic. It is observed that the low-frequency torque ripples are reduced in the case of shifted rotor motor.

3.3.4 Suitability for reverse motoring

Because of the symmetrical structure of the rotor with respect to the CCW and CW orientations, the proposed design modification is also suitable to reduce the torque ripple for the reverse direction of rotation. However, in the case of reverse motoring, the 0° rotor position in the modified motor changes to $(36^{\circ} \times n - 2.5^{\circ})$ of the forward motoring, where n is a positive integer number. The performance of the proposed motor is simulated for the reverse direction of rotation at rated speed and the results are given in Table 3.2. In

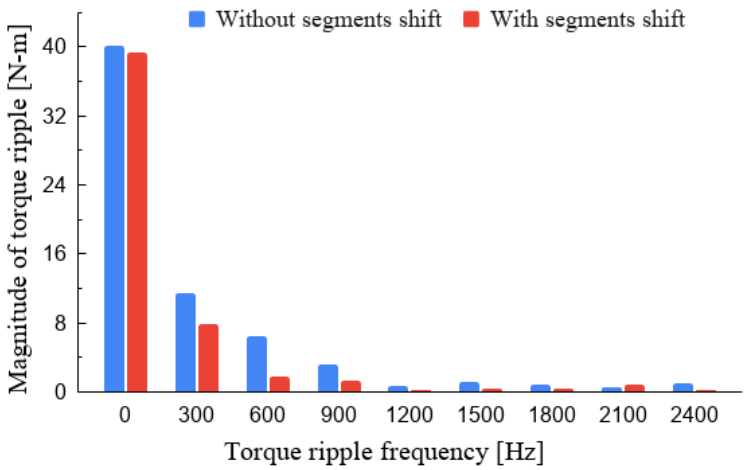

Figure 3.12: Comparison of torque ripple harmonics showing the reduction in lower order torque harmonics with the segment shift.

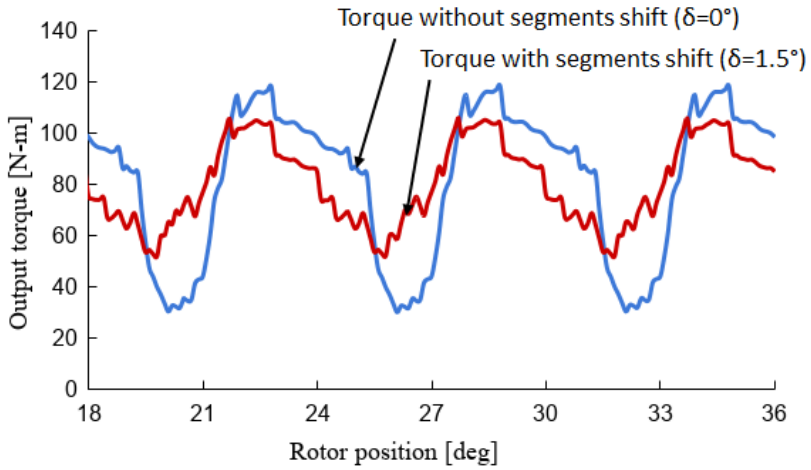

Figure 3.13: Comparison of steady-state torques of 24/20 pole DSSRM without and with rotor segments shift.

this case, the output torque and torque ripple for the proposed motor is 39.3 N-m and 47.3%, respectively, with approximately 40% reduction in torque ripple. These values are nearly the same as in the case of forward motoring as given in Table 3.1. The losses and rated efficiency are also comparable.

3.3.5 Segments shift in 24/20 pole DSSRM

It is discussed in Section 2.4 of the previous chapter that 24/20 slot/segment combination also has a high torque ripple. Therefore, the suitability of rotor segments shift to reduce the torque ripple is also checked for this motor, which has multiplicity $m = 4$. The design

Table 3.2: Performance data for reverse motoring.

Parameter	Without segment shift ($\delta = 0^\circ$)	With segments shift ($\delta = 2.5^\circ$)
Output torque	40.0 N-m	39.3 N-m
Peak-to-peak torque riple	31.4 N-m	18.5 N-m
Torque ripple	78.5%	47.1%
Reduction in torque ripple	-	40%
Reduction in output torque	-	2%
Core loss	53 W	60 W
Copper loss	362 W	363 W
Rated efficiency	85.8%	85.4%

Table 3.3: Performance data for 24/20 pole DSSRM without and with rotor segments shift.

Parameter	Without segment shift ($\delta = 0^\circ$)	With segments shift ($\delta = 1.5^\circ$)
Rated speed	600 rpm	600 rpm
Output torque	81.3 N-m	80.2 N-m
Torque ripple	108.4%	65.9%
Reduction in torque ripple	-	39.2%
Reduction in output torque	-	1.4%
Core loss	297 W	334 W
Copper loss	394 W	396 W
Rated efficiency	88.0%	87.3%

data of this motor is same as listed in Table 2.8. The steady-state response of the motor is simulated with the segments shift at the rated speed of 600 rpm. The minimum torque ripple is achieved for the value of $\delta = 1.5^{\circ}$. Fig. 3.13 shows the comparison of the steady-state torque waveforms without and with rotor segments shift. It can be seen that the torque ripple is reduced in the case of segments shift. Table 3.3 contains the performance data for 24/20 pole DSSRM without and with rotor segments shift at the rated speed. It is observed that torque ripple is reduced by 39.2% in the modified motor; however, the average torque is also reduced by 1.4%. Efficiency is decreased slightly in the case of shifted rotor motor because of the increase in core losses.

3.4 Torque ripple reduction through stator/rotor surface shift

In this subsection, the angular shift of stator and rotor surfaces have been investigated to reduce the torque ripples in DSSRM. The investigation is carried out with the individual shift of rotor and stator surfaces, firstly, and then simultaneous shift of stator-rotor surfaces. The total shift angle (δ_t) is as defined below.

$$\delta_t = (\delta_r - \delta_s) \tag{3.1}$$

where δ_r and δ_s are the shift angle of rotor and stator surfaces, respectively.

3.4.1 Rotor surface shift

In DSSRM, the rotor has two surfaces, inner and outer, which go through the magnetic flux influence. Therefore, the effect of individual inner and outer surface shift; and thereafter both surface shift are investigated. Fig. 3.14 represents the rotor's inner surface, outer surface and both surface shift, respectively. It is observed in the simulation results that shifting of rotor surfaces in the direction of rotation increases the torque generation capability of the incoming phase near unaligned rotor position. The sum of the static phase torques of the outgoing and incoming phases of 12/10 pole motor is obtained considering the commutation effect. It is considered that just after commutating the outgoing phase, its torque production becomes negligible.

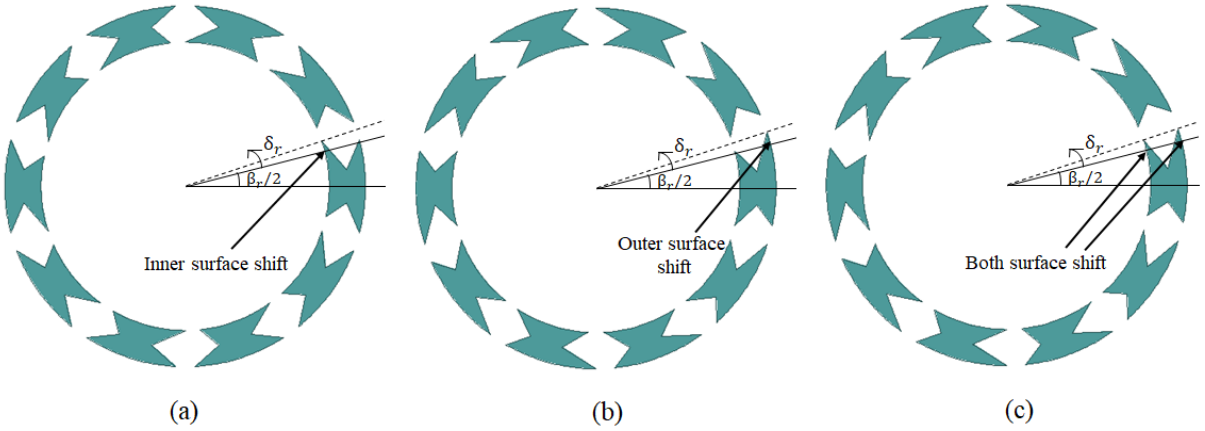

Figure 3.14: Shifting of rotor surfaces. (a) Rotor's inner surface shift. (b) Rotor's outer surface shift. (c) Rotor's both surface shift

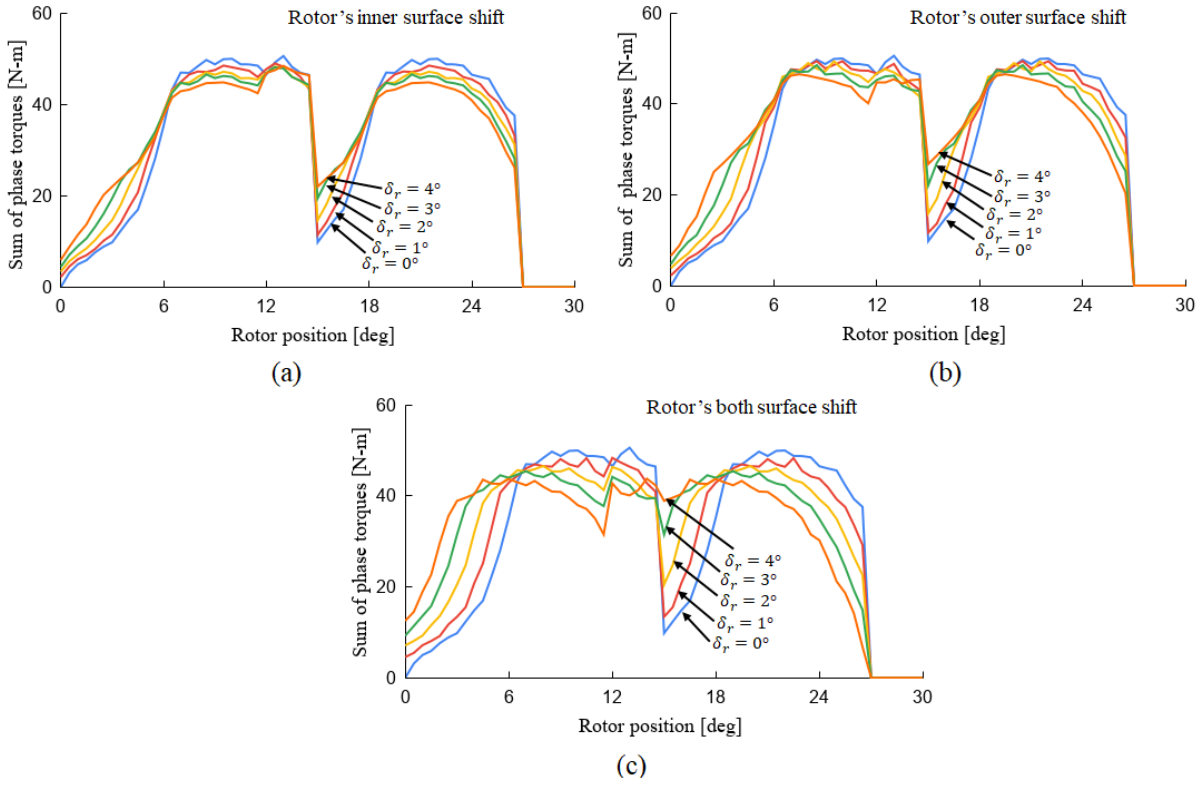

Figure 3.15: Reduction in torque dip in commutation region due to rotor surface shift. (a) Inner surface shift. (b) Outer surface shift. (c) Both surface shift.

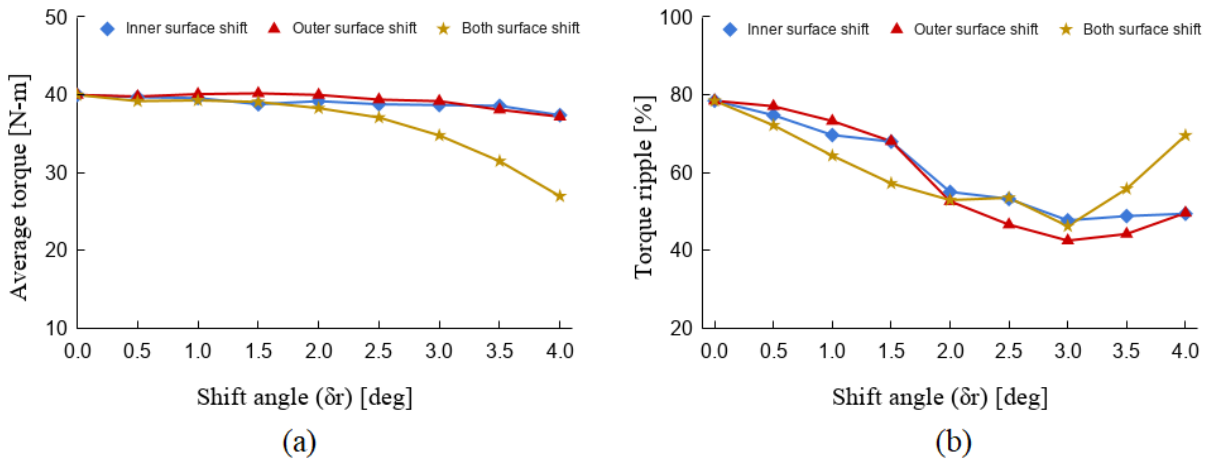

Figure 3.16: Variation of average torque and torque ripple with rotor surface shift angle (δ_r). (a) Average torque. (b) Torque ripple.

Fig. 3.15 shows the sum of the outgoing and incoming phase torques with the incremental shift in rotor's inner surface, outer surface and both surface, respectively, for 12/10 pole motor. It is observed that with the increase in shit angle (δ_r) the torque dip reduces in the commutation region. It is also observed that shifting of outer rotor surface is relatively more effective than inner surface to reduce the torque dip. Similarly, shifting of both surfaces is dominant over the inner as well as outer surface shift. However, these are static profiles, therefore, the dynamic responses are simulated at the rated speed to achieve more efficient results. Fig. 3.16 shows the variation of average torque and torque ripple with the variation of shift angle δ_r obtained through the dynamic response. The phase turn-on and turn-off angles considered are 0° and 14.5°, respectively. This figure prevails that the shift in the rotor's both surfaces provides the effective torque ripple reduction till $\delta_r = 2°$. However, the further increment in δ_r reduces the output torque significantly. Therefore, the reduction in torque ripple becomes less effective. The minimum torque ripple is obtained, in the case of rotor's outer surface shift with $\delta_r = 3°$. In this case, output torque (T_{avg}) and torque ripple (T_{ripple}) are 39.2 N-m and 42.6%, respectively. The values of T_{avg} and T_{ripple} are 40.1 N-m and 78.5%, respectively, without any surface shift. Therefore, torque ripple is reduced by 45.7%. However, the average torque also reduces by 2.2%. Table 3.4 deals with the comparative data for these surface shift. It is concluded from Fig. 3.16 and Table 3.4 that shifting of rotor's outer surface is more effective than the inner or both surface shift in the view of torque ripple and average output torque.

Table 3.4: Comparative data for rotor surface shift.

Parameter	Inner surface shift	Outer surface shift	Both surface shift
Shift angle δ_r for min T_{ripple}	3°	3°	3°
Min T_{ripple}	47.8%	42.6%	46.3%
% reduction in T_{ripple}	39.1%	45.7%	41.0%
Average torque T_{avg}	38.7 N-m	39.2 N-m	34.8 N-m
% reduction in output torque	3.5%	2.2%	13.2%

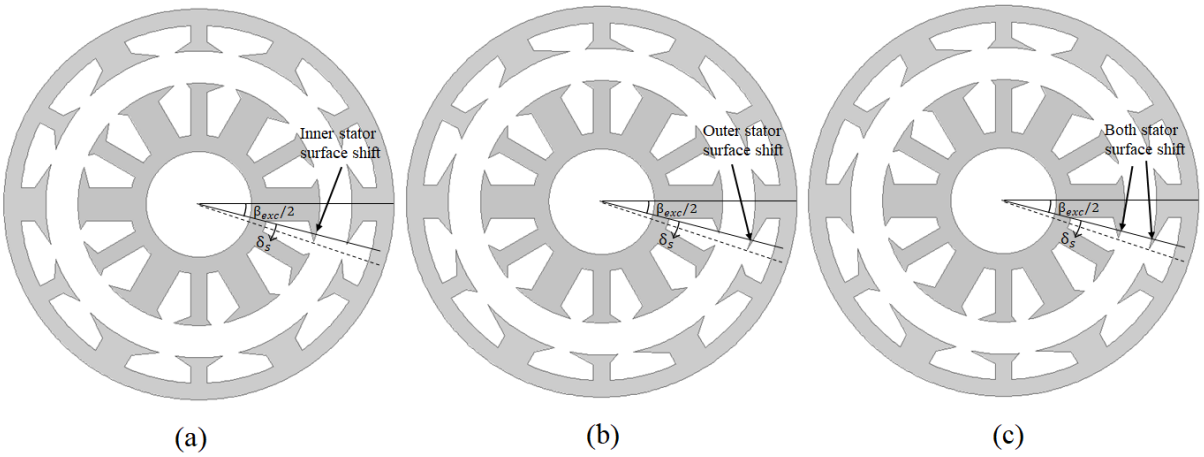

Figure 3.17: Shifting of stator surfaces. (a) Inner stator surface shift. (b) Outer stator surface shift. (c) Both stator surface shift.

3.4.2 Stator surface shift

The shifting of stator surfaces opposite to the direction of rotation also enhances the torque production of the incoming phase near unaligned rotor position. Therefore, it can also reduce the torque dip in the commutation region. Fig. 3.17 shows the pictorial representation of the inner stator, outer stator and both stators' surface shift, respectively, with the shift angle δ_s. Fig. 3.18 shows the sum of the static torques of the outgoing and incoming phase with the shift in inner, outer and both stator surfaces, respectively, for 12/10 pole motor. The shift angle of stator surfaces (δ_s) is considered in the step of -1°. It is observed that with the decrease in δ_s, the torque dip reduces. This concludes that shifting of stators' surfaces opposite to the rotation can effectively reduce the torque ripple in DSSRM. It is also observed from the static torque profiles, as shown in Fig. 3.18,

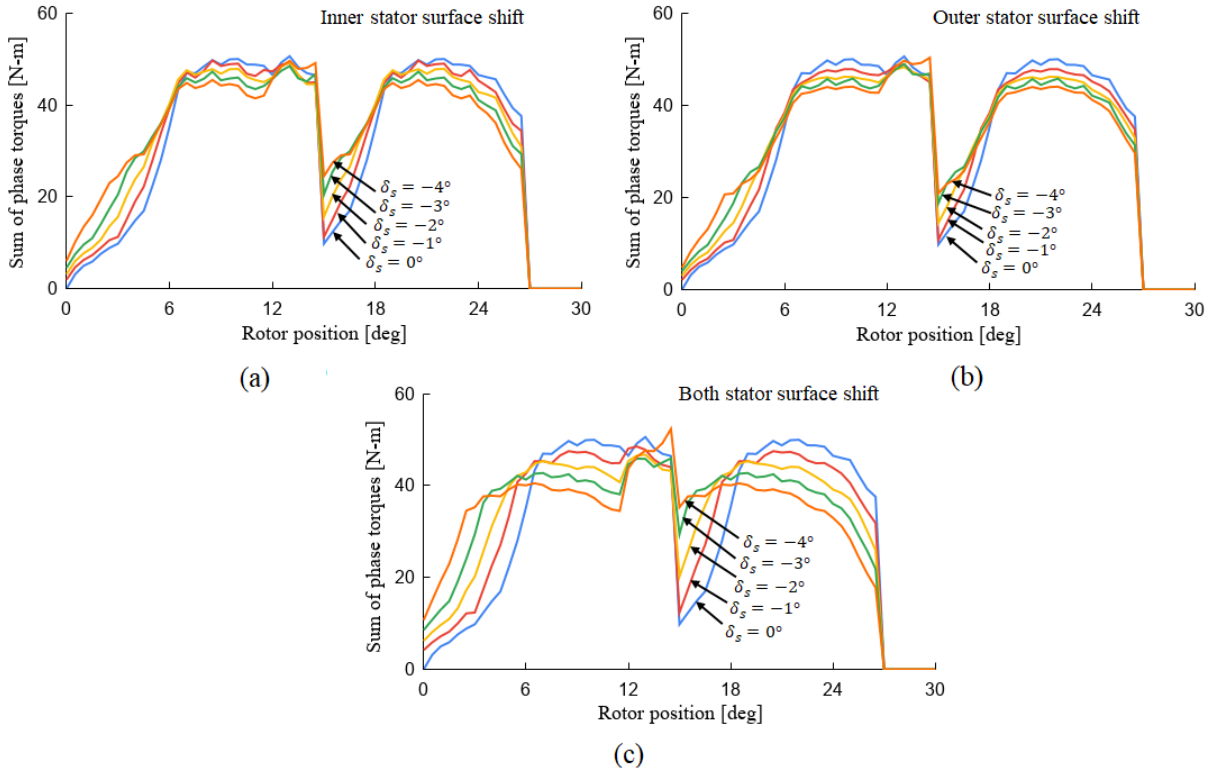

Figure 3.18: Reduction in torque dip due to stator surface shift. (a) Inner stator surface shift. (b) Outer stator surface shift. (c) Both stator surface shift.

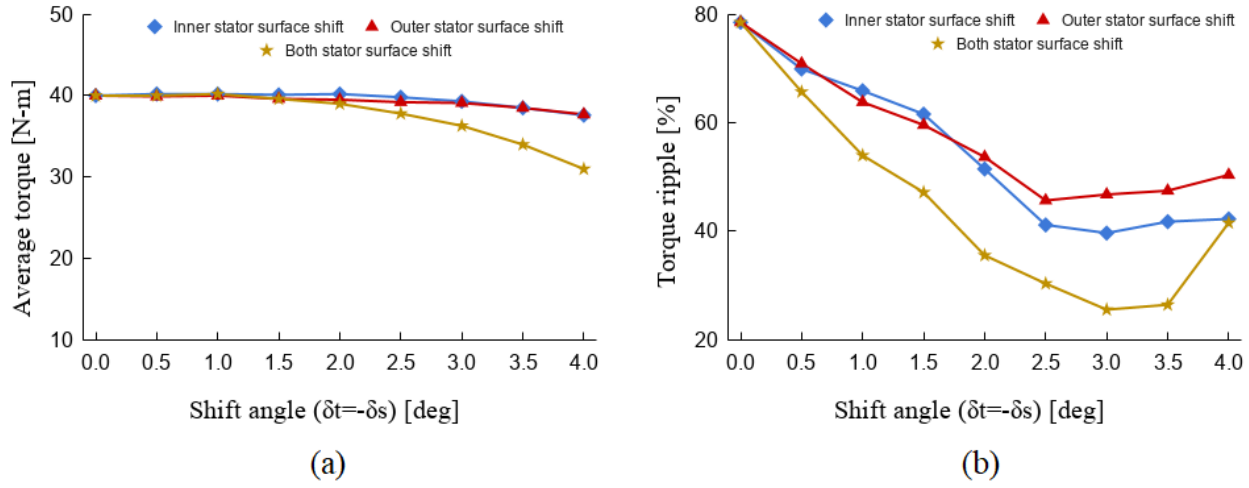

Figure 3.19: Variation of average torque and torque ripple with δ_t (where $\delta_t = -\delta_s$). (a) Average torque. (b) Torque ripple.

Table 3.5: Comparative data for stator surface shift.

Parameter	Inner stator surface shift	Outer stator surface shift	Both stator surface shift
Shift angle δ_s for min T_{ripple}	-3°	-2.5°	-2°
Min T_{ripple}	39.7%	45.7%	35.6%
% reduction in T_{ripple}	49.4%	41.8%	54.6%
Average torque T_{avg}	39.3 N-m	39.2 N-m	39.0 N-m
% reduction in output torque	2.0%	2.2%	2.7%

that shifting of both the stators' surfaces can reduce torque ripple more effectively than only one stator surface shift. However, for more precise analysis, the dynamic responses are simulated for shifted stator DSSRMs at the rated speed, and results are shown in Fig. 3.19. In Fig. 3.19, the variation of average torque and torque ripple are shown with the variation of shift angle. It is observed in the figure that shifting of both inner and outer stator surfaces can reduce the torque ripple more effectively. During the surface shift, the constraint considered is that the average torque should not reduce more than 3% of the rated value. Considering this constraint, the minimum torque ripple is achieved when both stators' surface shifted with $\delta_s = -2°$. The average torque (T_{avg}) and torque ripple (T_{ripple}), in this case, are 39.0 N-m and 35.6%, respectively. Therefore, torque ripple is reduced 54.6%, however, the average torque is also reduced by 2.7%. Table 3.5 deals with the comparative data for the stators' surface shift.

3.4.3 Stator-rotor surface shift

In the previous subsections, the shifting of rotor and stator surfaces are investigated to reduce the torque ripple in DSSRM. These investigations envisage that shifting of rotor's outer surface and shifting of both inner and outer stator surfaces effectively reduce the torque ripple in DSSRM. In this subsection, the effect of the simultaneous shift of stator and rotor surfaces are investigated. As per the results observed in previous subsections, in this case, only rotor's outer surface and both inner and outer stator's surfaces are considered for the simultaneous shift. Fig. 3.20 shows the simultaneous shift of stator and rotor surfaces. The stators' surfaces are shifted opposite to the direction of rotation,

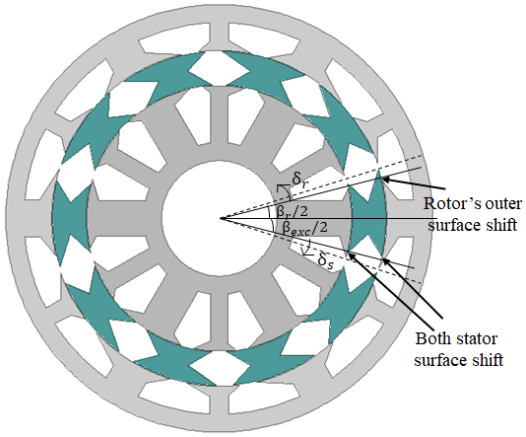

Figure 3.20: Stator-rotor surface shifted DSSRM.

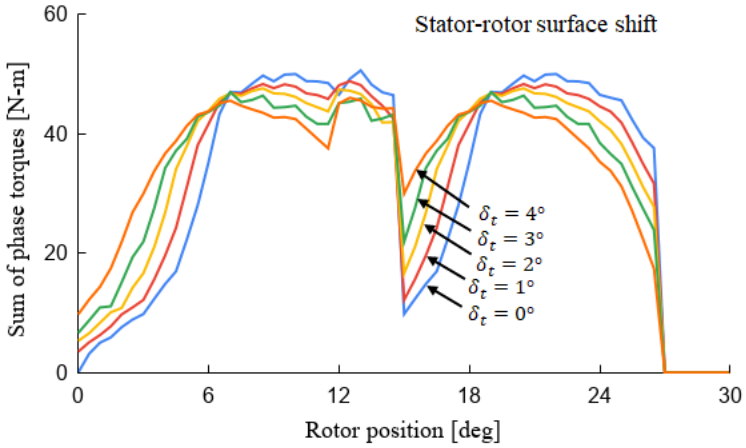

Figure 3.21: Reduction in torque dip due to stator-rotor surface shift.

whereas the rotor surface is shifted in the direction of rotation. The numerical values of δ_s and δ_r are considered same at an instant. The total shift angle (δ_t) is as given in Eq. (3.1). Fig. 3.21 shows the sum of static phase torques of the outgoing and incoming phases considering the commutation effect with the increment in δ_t by the step of 1°. It is observed that the increase in δ_t, leads to the reduction in torque dip. Dynamic responses are simulated at the rated speed and the variation of average torque and torque ripple with δ_t is shown in Fig. 3.22. The minimum torque ripple is obtained for $\delta_t = 2°$. In this case, the average torque (T_{avg}) and torque ripple (T_{ripple}) are 39.9 N-m and 45.9%, respectively. Therefore, the average torque and torque ripple are reduced by 0.5% and 41.5%, respectively.

Table 3.6 deals with the comparative data obtained in the above three sub-sections. The minimum torque ripple obtained is 35.6% for the shift of both the stator surfaces by

-2°. Therefore, it can be concluded that shifting of both inner and outer stator surfaces is best suited for the reduction of torque ripple in DSSRM.

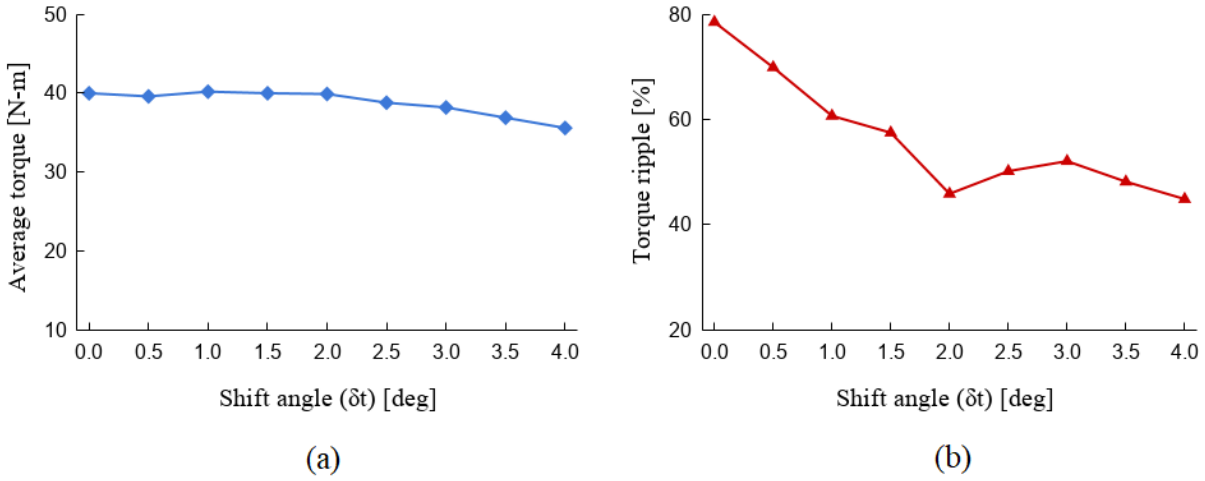

Figure 3.22: Variation of average torque and torque ripple with stator-rotor surface shift angle δ_t. (a) Average torque. (b) Torque ripple.

Table 3.6: Comparison of rotor, stator and stator-rotor surface shift.

Parameter	Rotor's outer surface shift	Both stators' surface shift	Stator-rotor surface shift
Shift angle δ_t for min T_{ripple}	3°	2°	2°
Min T_{ripple}	42.6%	35.6%	45.9%
% reduction in T_{ripple}	45.7%	54.6%	41.5%
Average torque T_{avg}	39.2 N-m	39.0 N-m	39.9 N-m
% reduction in output torque	2.2%	2.7%	0.5%

3.5 Conclusions

This chapter introduces the methods of torque ripple reduction in DSSRM via angular shift in the rotor segments as well as stator/rotor surfaces. Firstly, a schematic for torque ripple reduction is represented, thereafter segment and surface shift are investigated to

reduce the torque ripple using this schematic. From these investigations following conclusions are reached for the considered DSSRM topology.

- If the segment or surface is shifted in such a way that the incoming phase's torque increases near unaligned rotor position, the torque ripple can reduce effectively.
- Shifting of alternate rotor segments in the direction of rotation can effectively reduce the torque ripple.
- Shifting of rotor surfaces in the direction of rotation and shifting of stator surfaces opposite to the direction of rotation can effectively reduce the torque ripple in DSSRM.
- Shifting of both stator surfaces is dominant over other shifts to reduce the torque ripple in DSSRM.

The next chapter discusses about the influences of the segment and surface shift on the performances of the motor.